# Physical factors determining the fraction of stored energy recoverable from hydrothermal convection systems and conduction-dominated areas

by

Manuel Nathenson

U.S. Geological Survey

Menlo Park, California 94025

October, 1975

U.S. Geological Survey

Open-File Report 75-525

# INTRODUCTION

This report contains background analyses for the estimates of Nathenson and Muffler (1975) of geothermal resources in hydrothermal convection systems and conduction-dominated areas. The first section discusses heat and fluid recharge potential of geothermal reservoirs. The second section analyzes the physical factors that determine the fraction of stored energy obtainable at the surface from a geothermal reservoir. Conversion of heat to electricity and the use of geothermal energy for direct-heating applications are discussed in the last two sections.

# RECHARGE POTENTIAL OF GEOTHERMAL RESERVOIRS

The objective of this section is to compare the rates of natural heat discharge from geothermal reservoirs to expected levels of production in order to establish the conditions under which recharge of heat is important. The schematic diagram shown in figure 1 shows the important elements of a geothermal system. A reservoir is that region of hot rock with or without water which is being exploited in some fashion by wells with a total mass flow $m_p$. Hot recharge water of mass flow $m_h$ may enter the reservoir carrying its stored heat, and energy may enter the reservoir by conduction at the rate q. Cold water may flow into the reservoir at rate $m_c$ from the surrounding aquifer and additional water may be added by injection wells at a rate $m_i$. In the natural pre-production state, the mass flow of cold water and hot recharge water balances the natural discharge $m_d$. If we assume that cold water flow carries no energy above the reference state, the heat input by the hot water and conduction is balanced by the thermal water discharge $m_d$ and conducted heat output $q_d$. In the various reservoir types, not all of the elements shown in figure 1 are important.

Vapor-dominated reservoirs such as the ones at Larderello, Italy and The Geysers, California in their natural state are nearly closed systems to mass flows; leakage of vapor out of the reservoir is small compared to production but is significant as a mechanism for venting non-condensable gases. The sub-hydrostatic reservoir pressures (Truesdell and White, 1973) indicate that natural recharge of surface water must be less than the natural discharge; otherwise the system would collapse to a hot-water system. It is not known whether, in the natural state, discharge was being balanced by recharge or whether the systems were slowly depleting themselves of stored water.

Heat flows measured in the rocks above a vapor-dominated reservoir are from 6 to 15 $\mu cal/cm^2$ sec over large areas where there is no natural steam venting (Boldizsar, 1963, Urban and others, 1975) but convective losses within the small natural vent areas range up to thousands of $\mu cal/cm^2$ sec (White and others, 1971). Assuming that production will be on the order of 50000 kg/hr per well at an enthalpy about 640 cal/g above surface temperature and that wells will be sited on about 20 acres, the rate of energy removal is equivalent to 11000 $\mu cal/cm^2$ sec. The natural surface heat discharge over most of the reservoir is thus three orders of magnitude smaller than the rate at which heat is being removed by wells and the potential heat recharge may safely be neglected in calculating resource potential.

Hot-water reservoirs comprise a whole spectrum of types depending on the amount of natural heat and mass through-put and potential for cold-water recharge. At the extreme high end of this spectrum are systems like the one at Wairakei, New Zealand where natural convective

heat flow (Fisher, 1964) over the area of the hot part of the reservoir is equivalent to 900 $\mu cal/cm^2$ sec. The outflow of this heat at the surface was dominantly in the form of discharge from thermal features (hot springs, geysers and steaming ground). The source of this heat is a flow of deep water of essentially uniform composition up through the bottom of the reservoir. This deep water of meteoric origin circulates to great depths to pick up its energy. From the measured composition of reservoir water at Wairakei, it has been shown that a flow of 440 kg/sec of deep chloride water supplied the reservoir with its natural heat discharge. The current rate of exploitation of Wairakei is about 1600 kg/sec supplying 411 x $10^6 \frac{cal}{sec}$ of thermal energy (Axtmann, 1975) which is only about four times the natural discharge of heat, therefore the natural recharge potential of heat in the form of hot water is a significant fraction of production at Wairakei. It is not known whether the rate of natural heat recharge has been increased through exploitation, but there is little doubt that a significant fraction of the produced energy is being supplied by this recharge energy.

Parts of the system shown in figure 1 are the contiguous aquifers of warm and cold water supplying the reservoir with additional water. Cold water inflow is clearly happening in the exploitation of Wairakei where a comparison of the map of the gravity change caused by mass withdrawal (Hunt, 1970) with a map of subsurface temperatures (Banwell, 1963) shows significant removal of water from zones outside the high temperature area; Wairakei must have had significant cold water recharge during exploitation, even though no evidence for this cold recharge is yet evident in declining temperatures.

The other end of the spectrum of hot-water reservoirs is exemplified by the East Mesa system in Imperial Valley, California. This reservoir has no surface mass discharge and may simply involve a convection cell with no net through-flow of water. The measured natural heat flow is nowhere higher than 8 $\mu cal/cm^2$ sec (U.S. Bureau of Reclamation, 1974). A hot water well of 40 kg/sec flow with enthalpy of 200 cal/g on 20 acre spacing is equivalent to a heat flow of about 10 000 $\mu cal/cm^2$ sec, and this leads to the characterization that the natural heat flow is negligible compared to a reasonable production rate. Flows of water across the reservoir boundary during exploitation could be important but the natural flow of heat indicates that the heat recharge potential may be neglected.

A third type of reservoir is that in which permeability is low enough for no fluid circulation to take place--"hot dry rock". One may thus look at areas of the United States with conductive heat flow as being geothermal reservoirs, though it is likely that special places will have to be sought where the heat flow is above normal to exploit this resource. The major characteristics of such reservoirs are that (in the extreme limit) they have no natural fluid flow and simply conductive heat flow through them. Conductive heat flows can be not more than a few $\mu cal/cm^2$ sec unless magma is very close to the surface (Diment and others, 1975); since the equivalent heat flow of a producing well in a hot dry rock system would be of order $10^3$ $\mu cal/ cm^2$ sec, the heat recharge may also be neglected in hot rock resources.

In summary, except for a few systems with high convective flow of heat, the natural rate of heat discharge is much smaller than the rate

at which geothermal energy is likely to be produced. The process of extracting geothermal energy is thus one of extracting stored thermal energy from a body of rock and fluids. For purposes of resource calculation, the conductive flow of heat into the reservoir may always be neglected while the convective flow of heat may usually be neglected except in a few special cases. The flow of cold recharge water depends on the particular system and may range from a very small fraction of production to being equal to production.

## PHYSICAL FACTORS THAT DETERMINE THE FRACTION OF STORED ENERGY OBTAINABLE AT THE SURFACE

The purpose of this section is to isolate and analyze some of the important physical factors that generally limit the fraction of stored energy obtained at the surface. I will usually deal with uniform isotropic media, although the earth is rarely uniform or isotropic, and the response of a particular geothermal reservoir to production involves many factors peculiar to that reservoir. For example, the reservoir at Wairakei may be viewed as a body of porous fractured rock with low permeability boundaries at the top and bottom (Mercer, 1974, Donaldson, written communication, 1974). Both of these boundaries have local zones of faults or fractures of high permeability where recharge of deep hot water and discharge of near-surface thermal water cross the boundaries (Donaldson, written communication, 1974). One of the important properties of the reservoir (Waiora formation) is that its contact with the "impermeable" rocks at the bottom (Wairakei ignimbrites) is a zone of much higher permeability than occurs elsewhere in the reservoir (Grindley, 1965, Donaldson, written communication, 1974). Although many aspects of

a reservoir may be analyzed in terms of uniform isotropic media of simple geometry, the accurate prediction of response to production must include these complications.

Boiling in a hydrothermal system

The process of boiling of liquid water to steam can be important in vapor-dominated reservoirs and closed-volume hot-water systems (i.e. reservoirs in which production of mass is much greater than recharge). Figure 2 is a schematic representation of some boiling processes in a reservoir which was initially filled with hot-water and that is assumed to have no recharge. Figure 2 (top) shows the region in the immediate vicinity of a well in the early production stages. The boiling process involves a zone which moves with time to produce ever larger volumes of dry steam. The fundamental assumption here is that the liquid is moving slowly compared to the speed that the boiling zone moves. At later times, the process of gravity segregation would lead to the situation shown in figure 2 (bottom). The upper zone is a cap of dry steam underlain by a boiling zone and then a zone of liquid water. If wells fully penetrate the reservoir, the near-well region would be a combination of these two pictures. In systems with high recharge of cold or hot water, this picture is not true; the liquid would rise to maintain its pressure and prevent the formation of a steam zone. The ratio of recharge to production governs which part of a spectrum of behavior would occur. If recharge were equal to discharge, the boiling front would become stationary. No heat could then be obtained from the rock in the boiling zone and the system would produce a steam water mixture of constant total enthalpy as long as the supply of hot water lasted. In systems with moderately high

recharge potential, a steam zone may be created by withdrawing mass from both the steam and water zones in order to keep the boiling zone moving and prevent collapse of the steam zone, (James, 1968).

In the idealized system of figure 2 in which the liquid moves much slower than a propagating boiling zone, we can analyze the overall response of the system by simply looking at initial and final states across the zone (see Truesdell and White, 1973, Bodvarsson, 1974). Assuming the boiling zone to be of constant but arbitrary thickness, and neglecting heat conduction, conservation of energy may be written as

$$[\rho_r(1-\phi)c_r(T_o-T_1) + \rho_{wo}\phi h_{wo}]\dot{\ell} = \rho_{g1}\phi h_{g1}\, U \qquad (1)$$

where the subscript r refers to rock of density $\rho_r$, specific heat $c_r$, and porosity $\phi$. The rock is initially at temperature $T_o$ and changes to a final temperature $T_1$ on the steam side of the zone. The front moves with velocity $\dot{\ell}$ vaporizing an amount of water $\rho_{wo}\phi\dot{\ell}$ to produce a flow of saturated steam of $\rho_{g1}\phi U$. By continuity, we have $\rho_{g1}\phi U = \rho_{wo}\phi\dot{\ell}$, and equation (1) may be rewritten as

$$\rho_r(1-\phi)c_r(T_o-T_1) + \rho_{wo}\phi h_{wo} = \rho_{wo}\phi h_{g1} \qquad (2)$$

as the equation connecting the initial and final states across the zone. Equation (2) is nonlinear in that the enthalpy of steam and water as a function of temperature is required to solve it, but the equation may be solved easily using iteration with the steam table data (Keenan and others, 1969). (For a given value of $T_o$, the procedure is to guess $h_g$, solve for $T_1$, get a new $h_g$ from the steam tables, and calculate a new $T_1$. The pressure at 1 is the saturated vapor pressure at the temperature $T_1$. Since $h_g$ is a weak function of temperature, the procedure is rapidly convergent.) Figure 3 shows plots of final pressure and final temperature

at the steam end of the boiling zone as a function of initial temperature for various values of porosity. An important lower limit to when a geothermal reservoir may be produced using this mechanism is that the final pressure must be high enough to be able to push the steam through the porous media and up the well at a significant rate. Based on the calculations of Nathenson (1975), a reasonable assumption as to this lower pressure limit is 8 bars absolute pressure. The curves in figure 3 are drawn as broken lines in the region where final pressures are below 8 bars.

The fraction of energy recovered by this boiling process depends on a number of factors. Assuming the ideal process shown in figure 2 (bottom), the passage through porous rock of initially saturated steam with decreasing pressure is nearly an isothermal process leading to increased enthalpy and superheating the steam. In order to simplify the recovery calculation, the steam is assumed to leave as saturated steam at the final state shown in figure 3. The thermal energy per unit mass of steam is then $h_{g1}$ less the enthalpy of saturated liquid at 15°C $h_{w15°C}$. The fraction of stored thermal energy above 15°C which may be obtained at the surface may be written as

$$e = \frac{\rho_{wo}\phi\ (h_{g1} - h_{w15°C})}{\rho_r(1-\phi)c_r(T_o-15°C) + \rho_{wo}\phi\ (h_{wo}-h_{w15°C})}\ e' \qquad (3)$$

where the denominator is the energy stored per unit volume in the rock and the water and the numerator is the initial mass of water per unit volume times the thermal energy per mass of fluids. The factor $e'$ is a recovery factor to allow for nonideal reservoir behavior and abandonment pressure being something above zero. It is not really known what value

$e'$ takes in a real field. For hot-water systems, the value of $e'$ is partly a function of the porosity and initial temperature. This dependency is caused by a field having to be abandoned at some pressure above zero; the higher the final pressure shown in figure 3, the higher the recovery factor $e'$ is expected to be. Figure 4 shows the fraction of stored energy obtained at the surface for unit recovery $e' = 1$ (see equation (3)). The parts of the curves which are broken show where the final pressure is less than 8 bars. The curves are relatively flat, indicating recoverability fractions which are not very dependent on temperature, but the final pressure limitation shows that over a significant range of porosity and temperature, this technique is not applicable, so the recovery factor would be zero.

Vapor-dominated systems

Vapor-dominated systems may be related to the above considerations by the model shown in figure 5 (Truesdell and White, 1973). The initial state of the reservoir is a two zone system comprised of a deep zone saturated with liquid water and an upper zone with steam as the pressure controlling phase and containing liquid water immobilized in the pores by surface tension forces. After a well has produced for some time, it is surrounded by a region of reduced pressure and consequently of dry steam. Beyond this dry-steam is a region where immobilized pore water responds to the lowered pressure by boiling to saturated steam using the energy in the rock to provide the heat of vaporization. In the deep part of the system, there is likely to be a brine saturated zone also boiling to provide new steam. Neglecting a second order correction, the curves in figures 3 and 4 may be used for vapor-dominated reservoirs if

the average water content in the total reservoir volume, which is the product of the actual porosity and the fraction of pores which are filled with liquid water, is used for the porosity. Thus a vapor-dominated system with 0.1 porosity and 0.1 of the pores filled with liquid water will have a final pressure and temperature from the curve in figure 3 marked $\phi = 0.01$. From figure 3, this kind of value implies small temperature changes in the boiling process. The fraction of energy recovered obtained from figure 4 for this case is 0.04. The recovery factor $e'$ in equation (3) is likely to be close to one since the small quantities of water to be boiled make final pressures at the end of boiling significantly above 8 bars.

Cold water drive

The next recovery technique to be discussed is a sweep process of using cold water to drive hot water in a reservoir. The drive may be provided either by natural cold-water recharge or the injection of cooled formation water. Because of legal limitations on the discharge of mineralized water to surface waters, it is likely that injection will be required in most areas. Except in special circumstances, this injection will be into some part of the geothermal reservoir or into a contiguous aquifer. Although, the prediction of the behavior of such systems is complicated and should be done using reservoir simulators (see for example Mercer and others, 1975), it is possible to analyze in a simple manner several of the important physical factors which govern and limit the fraction of stored energy which may be recovered in a sweep process. Three types of physical problems will be discussed: 1) The spreading as a function of time of an initial discontinuity of temperature caused by

heat conduction with no fluid movement. The point is to show that the diffusion of temperature takes place over a small enough length scale, that it may be superimposed in analyzing a sweep process which takes place in an aquifer that is longer and thicker than the conduction length. 2) Sweep in the horizontal plane. This involves considerations of flow pattern in a linear flood and in a five spot drive (a repeated array of production wells set in a square of four injection wells). The important point is that a temperature front moves at a much lower velocity than the average pore velocity (the velocity of a chemically tagged fluid particle) and that large fractions of stored energy may be recovered under ideal conditions. 3) Movement in the vertical section of an initially vertical cold-hot water interface due to gravity segregation. In a real reservoir, these processes are coupled and operate simultaneously. I assume that the equations are sufficiently linear that they may be superimposed to a first approximation.

The first problem is heat conduction in a uniform medium of thermal conductivity $k_{Th}$, volumetric specific heat $\rho c = \phi\rho_w c_w + (1-\phi)\rho_r c_r$, and diffusivity $\alpha = k_{Th}/\rho c$. The initial temperature distribution is assumed to be a step change in temperature and the solution is obtained in terms of error functions (see for example Rosenhow and Choi, 1961, p. 119-121). The interest here is in the conduction length X defined as the length over which significant conduction effects take place. From the solution, we obtain $X = 4(\alpha t)^{1/2}$. Assuming 5 mcal/cm sec°C thermal conductivity and 0.68 cal/cm$^3$°C volumetric specific heat (20% porosity and 0.6 cal/cm$^3$°C specific heat for the solid), the diffusivity $\alpha$ is 23.2 m$^2$/yr. The conduction length as a function of time is given in

table 1. From these values, a scale of interest of a few hundred meters or more relegates conduction effects to a boundary layer structure in regions of high temperature gradient on the order of tens of meters thick for time scales on the order of a decade. If we have a front that is to move say one kilometre in an aquifer 500 metres thick, conduction effects are restricted to thin regions compared to the vertical and horizontal dimensions. This assumption will be used in the following to superimpose conduction effects on sweep front solutions.

The second problem is to look at various flood processes of cold water sweeping into a hot saturated porous medium (see Bodvarsson, 1972 and 1974 for similar discussions). The governing equations for two dimensional horizontal flow are

$$\frac{\partial q_x}{\partial x} + \frac{\partial q_y}{\partial y} = 0 \tag{4a}$$

$$q_x = \frac{-k}{\mu} \frac{\partial p}{\partial x} \quad q_y = \frac{-k}{\mu} \frac{\partial p}{\partial y} \tag{4b}$$

$$[\phi \rho_w c_{vw} + (1-\phi)\rho_r c_r] \frac{\partial T}{\partial t} + \rho_w c_{vw}[q_x \frac{\partial T}{\partial x} + q_y \frac{\partial T}{\partial y}] = k_m \left( \frac{\partial^2 T}{\partial x^2} + \frac{\partial^2 T}{\partial y^2} \right) \tag{4c}$$

where $q_i = \phi V_i$, $q_i$ is the seepage velocity, $V_i$ is the pore velocity, k is the permeability, $\mu$ is the viscosity, and $k_m$ is the mixture thermal conductivity and water and rock are assumed to be locally at the same temperature. The enhancement of thermal conductivity by hydrodynamic dispersion will be neglected. Using the assumption that conduction effects are restricted to thin regions compared to the problem domain, equation (4c) may be written approximately as

$$\phi^* \frac{\partial T}{\partial t} + q_x \frac{\partial T}{\partial x} + q_y \frac{\partial T}{\partial y} = 0 \tag{5a}$$

$$\phi^* = \phi + (1-\phi)\frac{\rho_r c_r}{\rho_w c_{vw}} \tag{5b}$$

The fundamental solution to equation (5a) for a moving front is

$$T(x,y,t) = T(x-q_x\, t/\phi^*,\ y-q_y\, t/\phi^*). \tag{6}$$

The meaning of equation (6) is that a line of constant temperature moves with a velocity $q_x/\phi^*$ in the x-direction and $q_y/\phi^*$ in the y-direction. Using volumetric specific heats for water of one and for rock of 0.6 cal/cm$^3$°C, we obtain $\phi^* = 0.6 + 0.4\phi$, so the quantity $1/\phi^*$ is between 1.5 and 1.7 for $0.2>\phi>0$. Thus temperature waves move at between 1.5 and 1.7 times the seepage velocity $q_i$ whereas waves of tagged fluid particles move at the average pore velocity $V_i$ which is greater than five times the seepage velocity. Thus one would expect isotopically tagged recharge water to show up at a production well long before a temperature change in an initially hot porous medium.

In the approximation that conduction effects are restricted to thin regions, the structure of equations (4a,b) and (5) is identical to that for miscible displacement processes. Thus analyses from petroleum and salt-water encroachment studies may be used for this kind of problem with concentration and porosity replaced by T and $\phi^*$. The first example is a linear displacement involving cold water injected at x=0 into an initially uniform hot aquifer. At some distance L from the injection point, the temperature front will arrive at time $t = \phi^* L/q_x$ and a volume of hot fluid per unit area of $\phi^* L$ will have been produced at the hot temperature. The fraction of stored energy recovered would be near one as long as the length L is much greater than the conduction lengths calculated above. Because the process involves using cold viscous water

to drive hot less viscous water, the mobility ratio $\mu_{hot}/\mu_{cold}$ is favorable (i.e., less than one) and temperature fronts are stable and will not finger (assuming that standard miscible displacement experiments are valid) (see for example Haberman, 1960).

The effect of conduction on the cold-water drive analysis may be superimposed in the linear displacement problem to produce the behavior shown in figure 6. The temperature distribution as a function of distance is shown at various times for a porosity of 0.2. The velocity of the thermal front is assumed to be 50 m/yr. Assuming a volumetric specific heat for water of 1 cal/cm$^3$°C and of rock of 0.6 cal/cm$^3$°C, we obtain $\phi^*$ = 0.68. The velocity of a chemically tagged fluid particle is then (0.68)(50 m/yr)/0.2 = 170 m/yr. At one and five years, the location of a chemical front is shown by a vertical broken line. At 9.4 years, the chemical front moves out of the diagram. As time passes, the initially sharp temperature front becomes more diffuse, and by 30 years has spread to about 100 meters in length. (Table 1).

Another horizontal-sweep geometry involves the possible application of the five-spot drive pattern (four injection wells surrounding a producing well) to recovering stored energy from a geothermal reservoir. As the temperature front nears the production well, the front gets sucked in. Figure 7 shows experimental data reproduced from Haberman (1960) for miscible displacement in one-fourth of a five spot (the pattern is the same in the other three quadrants). The top figure is for a mobility ratio of 0.151 corresponding to more than 200°C temperature difference and the bottom is for a mobility ratio of unity corresponding to a small temperature difference. The numbers shown are the

fraction of stored energy e which has been produced when the front is at the location shown while the number of pore volumes which have passed through the system is $e\rho_r c_r/\phi\rho_w c_w$. For $\phi = 0.2$ and $\rho_r c_r/\rho_w c_w = 0.6$, three times e is the number of pore volumes required to sweep the system. In the case of a five-spot array the neglect of heat conduction at the front is not good as an approximation. For a well lasting 30 years at a flow $10^6$ lb/hr and 40 acre spacing, the length of a side is 402 m and the aquifer thickness is about 1 km. The side length is relatively close to the conduction length so the spread of the front becomes important. However, the spread is also dependent on the geometry so the conduction lengths in table 1 are not quite applicable. If the aquifer were thinner, the well spacing would have to be greater to satisfy the volume requirements, and the relation between the conduction length and a side length would be closer to the assumed relation. The whole problem of the interplay between conduction and sweep in a five-spot array requires more detailed analysis, but the results of figure 7 show that the fraction of recoverable energy cannot be more than 0.6 or 0.7.

The third physical problem to be discussed is gravity segregation of miscible fluids in a vertical section. The physical situation involves cold water driving hot water in an aquifer thick enough to neglect conduction. Neglecting the mobility difference, the problem may be idealized to an initially vertical temperature discontinuity. As time goes on, the discontinuity will move in a direction toward horizontal with the heavy cold water moving into what was hot along the bottom half and the light hot water moving into what was cold along the top-half. The governing equations are similar to equations (4) and (5) with the

addition of a gravity term in the vertical component of Darcy's law and an equation relating fluid density and temperature. The equations neglecting heat conduction are identical to those for regular miscible displacement with $\phi^*$ from equation (5b) replacing the porosity. Gardner and others (1962) have presented data and analysis for miscible displacement. Using their curves to obtain the overall length for 250°C as high temperature and 50°C as low temperature, curves in figure 8 have been sketched for times of 15 and 30 years for 100 mdarcy and for a time of 30 years for 30 mdarcy permeability. For the lower permeability, the interface remains close to vertical. For the higher permeability model, cold water moving under the hot water is a significant potential problem. For thinner aquifers, the conductive heat transfer from beds above and below the aquifer would be important. Since these beds are hot, they would tend to retard the movement of the cold water interface.

The complexity of even these simple analyses indicates the difficulty of obtaining estimates of the fraction of stored energy which can be recovered. The simultaneous operation of these different physical processes combines with the effects of real geometry to make rigorous solutions impossible with available data. However, a subjective combination of the various factors suggests that, for the areal sweep problems, an overall recovery factor of 0.6 to 0.8 is reasonable. The processes of gravity segregation and shunting by permeable zones might lead to premature breakthrough and reduce the overall recovery factor to 0.3 to 0.5. On the average, perhaps 0.5 of the energy stored in a porous and permeable reservoir may be recovered through the use of a sweep process. This recovery factor undoubtedly will be refined as geothermal reservoirs are developed and as more complete analyses are performed.

Hot-dry rock

The next physical problem concerns hot-dry rock. A limiting case of the physical system is a vertical planar crack of negligible thickness with water which flows in the crack, absorbing heat only by conduction. Figure 9 shows an idealized problem of such a crack of height b and length b and negligible thickness. Whether there is one crack per pair of recharge and production wells (Harlow and Pracht, 1972) or a series of cracks per well pair created by slant drilling (Raleigh and others, 1974), there would still be a series of cracks spaced on an interval d to optimize the recovery of stored energy. It is likely that extracting energy from conduction dominated areas would take place in special places with favorable resource potential, so the fraction of stored energy recovered is important. The rock is initially at temperature $T_i$ and the rock has density $\rho_r$, specific heat $c_r$, conductivity $k_r$, and diffusivity $\alpha = k_r/\rho_r c_r$. The total mass flow rate of water introduced at temperature $T_o$ at x=y=0 into n cracks is qbn where q is the flow per unit length of crack. The solution to this problem for infinite crack spacings, neglecting edge effects, is given by Bodvarsson (1969, 1974). Defining a dimensionless group with the flow rate $\beta = 2k_r/c_w q$, the solution may be written as

$$\frac{T(x,y,t) - T_o}{T_i - T_o} = \operatorname{erf} \frac{\beta x + |y|}{2\sqrt{\alpha t}} \quad . \tag{7}$$

For finite crack spacing one may either use the solution of Gringarten and others (1975) or equation (7) with appropriate constraints. Bodvarsson (1974) suggests that the spacing may be set by making the perturbation in temperature at the midpoint (y = d/2) negligible by using equation

(7). This is confirmed by the demonstration of Gringarten and others (1975) that, after the conductive heat transfer of adjoining cracks starts to interact, temperatures rapidly decay with time. Assuming that a 5% temperature perturbation at (x = 0, y = d/2) is negligible, (erf $d/4(\alpha t)^{1/2} = 0.95$), we obtain

$$d/2 \geq 2.8\sqrt{\alpha t_f} \tag{8}$$

where $t_f$ is the time when the system is no longer usable. Setting $t_f$ = 30 years and $\alpha$ = 21 $m^2/yr$, we obtain d = 141 m. The maximum flow per unit length of crack q may be fixed by assuming a value for the exit temperature at time $t_f$ when the system will be abandoned. Assuming that a dimensionless temperature of 0.5 corresponds to abandonment, (erf $\beta b/2(\alpha t)^{1/2} = 0.5$), we obtain

$$\frac{q}{b} \leq \frac{k_r}{0.48 c_w \sqrt{\alpha t_f}} \tag{9}$$

Using the above values and $c_w$ = 1 cal/g°C, we obtain q/b = 3.32 x $10^{-6}$ g/sec $cm^2$. The fraction of stored energy recovered may be obtained by integrating over the rock volume the energy removed by changing the temperature from $T_i$ to the final temperature at time $t_f$ and dividing by the energy stored above the temperature $T_o$. This may be expressed as

$$e = \frac{q\, c_w t_f}{\rho_r c_r bd}\; A\left(\frac{\beta b}{2\sqrt{\alpha t_f}}\right) \tag{10}$$

where the function A is an integral of the error function given by Bodvarsson (1974). For the values given above, e = 0.26; thus a large fraction of the stored energy (~75%) remains in the ground at abandonment.

The analysis may be made more meaningful by applying it to a specific case. For a single crack 1 km long and high, like that of Harlow and Pracht (1972), the total flow from equation (9) is qb = 33.2 kg/sec.

Dimensional and dimensionless temperatures at the crack outlet are presented in the top of figure 10 for an assumed initial system of 200°C injected with 40°C water. Temperatures in the rock at 30 years are presented in the bottom of figure 10. Note that the horizontal axis is in metres while the vertical axis is dimensionless. For b = 1 km, the true shape of this figure is long in the vertical and short in the horizontal. The bottom figure provides a visual confirmation of the large amount of energy left in the rock. The top figure illustrates an important problem with this simple method of recovering energy. In order to recover a significant fraction of the stored energy, the temperature of the produced fluid decays quite a bit over the life of the system. Most utilization schemes can not tolerate a wide variation in temperature. Various possibilities suggest themselves to correct this problem such as topping to some average temperature and/or using variable flow rates to even out the temperature pattern.

To evaluate multicracks per well, we can fix the total flow qbn at 33.2 kg/sec. Since the value of q/b is determined by equation (9), we obtain $b^2n$ equal a constant i.e., total crack area is constant for constant total flow. For 5 cracks, we obtain b = 447 m and for 10 cracks, b = 316 m. Significant reductions in individual crack size are thus obtained in the multicrack geometry.

The analysis of recovering energy from hot rocks has been restricted here to the idealized conduction problem. Harlow and Pracht (1972) suggest that permeability and porosity will grow from cracking due to stress caused by thermal contraction. In this case, Harlow and Pracht's flow rate in their example 2 roughly corresponds to the present example

and the thermal power becomes nearly constant after a few years due to the growing region of created porosity. Their example 1 has a flow rate approximately four times the value used here, exhibits steep initial decline, but gives increasing power at late time as the porous region is created faster than the energy is extracted. In such schemes, the average spacing between cracks would, of course, have to be large enough to prevent interaction. It is not yet known which way rock will behave in response to cold water injection into a crack. If significant new porosity is not created, the limitations imposed by the conductive calculations are dominant and average flow per well is fixed. If new porosity is created, the average flow per well is determined by a whole range of interacting parameters.

Real reservoirs depend mainly on fracture permeability and may respond as a combination of flow through porous media and of conduction to water flowing in a crack. The analysis of a particular reservoir requires consideration of what process is dominant in what part of the reservoir.

## ELECTRIC POWER CYCLES

The choice of the optimum cycle for conversion of geothermal energy to electric power is dependent upon efficiency of conversion, cost, and special reservoir problems such as high dissolved solids, high gas contents, deposition of scale, etc. The purpose of this section is to calculate the energy produced per unit mass of reservoir fluid as a function of source enthalpy for pure steam, flashed steam, total flow, and binary isobutane cycles. The reference or final state to be used in these calculations is 40°C saturated liquid. Depending on local conditions,

lower final states may be obtainable. An important concept to be used is the availability which is defined by Jones and Hawkins (1960) as "the maximum amount of useful work which could be obtained from the system-atmosphere combination as the system goes from that state to the dead state while exchanging heat only with the atmosphere." Real cycles do not produce this maximum work, and their efficiencies are judged by how close they come to this ideal. Efficiency losses due to any necessary gas extractors will be neglected, though these can be very important when gas contents are high.

Steam

The simplest cycle is for pure steam, produced either by a vapor-dominated system or as the result of flash-separation of steam from residual water. Assuming the steam to be saturated, the enthalpy above 40°C is $h_{gl}-h_{wo}$ where gl denotes the initial saturated steam at temperature $T_1$ and wo denotes saturated liquid at temperature $T_o$ = 40°C. The conversion to electrical energy takes place in a turbine-generator set with an ideal turbine involving an isentropic expansion to wet steam at 40°C. The actual work may be computed from

$$w_{act} = [(h_{gl} - T_o s_{gl}) - (h_{wo} - T_o s_{wo})]\, e_t \qquad (11)$$

where the $e_t$ factor is to account for mechanical and other losses in the system and s is the entropy. The ideal maximum work (availability) is computed from equation(11) with $e_t$ = 1. For real turbines, an $e_t$ value of 0.7 for mechanical and other losses is reasonable (Austin and others, 1973). Heat above 40°C, availability, and actual work have been computed using steam table data (Keenan and others, 1969) and are shown as broken lines in figure 11. The unit used on the ordinate is kW·s/kg (=joule/

gram) for thermal or mechanical energy per unit mass of produced fluids. This unit may also be written as a $\frac{kW}{kg/sec}$, so the numbers in figure 11 may be multiplied by the mass flow in kg/sec to obtain the power in kW. For comparison, the actual output figure for units 5 and 6 at The Geysers (Finney, 1973, figure 2) are shown on the figure as a horizontal line spanning the range where the enthalpy of saturated steam is about the same as the superheated steam that is fed into the turbine. The Geysers' data show that the calculated work per unit mass is close to real value. (In analyzing steam turbines one should more properly do a cycle analysis and calculate the work output from an isentropic expansion from saturated steam at $T_1$ to wet steam at $T_o$ and apply $e_t$ to that number. Because the ideal steam turbine cycle is close to a Carnot cycle, the answers differ very little, and the present calculation method is adequate. This is not true when varying superheat is involved.) The efficiency of this system is only defined if it is made into a cycle, in which case it would be the work out divided by the heat in. For present purposes, a more useful factor $e_c$ is defined as the actual work divided by the enthalpy in the steam above a 15°C saturated liquid reference state. Since resource estimates are reported as energy above 15°C, this provides a convenient factor to convert recoverable heat to electrical equivelent, and this factor is plotted in figure 12.

Hot water

The more common fluid in geothermal reservoirs is liquid water and a number of schemes have been proposed to convert its thermal energy to electrical energy. Regardless of scheme, we can analyze the maximum work using the concept of availability. The heat above 40°C is $h_{w1}-h_{wo}$ where both symbols are for enthalpy of saturated liquid at the given

temperature. The availability for liquid water is

$$y = (h_{w1} - T_o s_{w1}) - (h_{wo} - T_o s_{wo}) \qquad (12)$$

where enthalpy and entropy are for saturated liquid at temperatures $T_{w1}$ and $T_o$ ($T_o$ in equation (12) is the absolute temperature). The utility of equation (12) is that it gives the maximum work of any process that is within the restrictions without having to specify a process. Values obtained for heat above 40°C and maximum work are shown in figure 11.

Single and double flash

The current technology for hot-water systems involves the flashing of liquid water to a steam-water mixture in a selfpumping well, sending the mixture through a separator where the steam is extracted from the water, and the steam fraction is then sent to the turbine. The water is then simply rejected taking significant amounts of availability with it. James (1968) has suggested that the two-phase mixture be sent to the powerhouse in a single pipe where the steam is separated rather than having the separation take place at the wellhead. It would then be very easy to have a second separation to obtain significantly greater net output. For any given reservoir enthalpy, there is an optimum pressure for separation to obtain maximum work per unit mass of fluids; however, the practical consideration of maximizing the flow from a well over a long period of reservoir depletion dictates that wellhead pressures be kept low (James, 1967). As a reasonable compromise, the pressure of first separation will be chosen as 6 bars absolute. Defining the mass fraction of steam at a separation pressure of $P_2$ = 6 bars as $N_1$ and assuming high enough flow for negligible heat losses in the well and neglecting kinetic energy, conservation of energy may be written as

$$h_{w1} = h_{w2} + N_1 h_{wg2} \tag{13}$$

where $h_{wg2}$ is the enthalpy of vaporization at 6 bars. The actual work per unit mass of reservoir fluid may be written as

$$W_{act} = N_1\{(h_{g2} - T_o\, s_{g2}) - (h_{wo} - T_o\, s_{wo})\}\, e_t \tag{14}$$

and the calculated values are shown in figure 11. For comparison, the actual value obtained at Wairakei, New Zealand is also shown (Axtmann, 1975).

For a two-stage flash, the first flashing still takes place at 6 bars. The temperature and pressure for the second flash are obtained by a trial-and-error optimization of the second-stage work. This optimization involves the competing factors of lowest pressure yielding the largest fraction of steam and the highest pressure yielding maximum work per unit mass of steam. The optimum temperature is found to be 97°C (0.9 bar abs.). The actual work per unit mass of reservoir fluid is

$$W_{act} = \{N_1\,[(h_{g2} - T_o\, s_{g2}) - (h_{wo} - T_o s_{wo})] + (1-N_1)N_2[(h_{g3} - T_o S_{g3}) - (h_{wo} - T_o\, s_{wo})]\}\, e_t \tag{15}$$

where $N_1$ is obtained from equation (13) and the subscript 3 refers to saturated steam at $T_3 = 97°C$. The mass fraction of second-stage steam is obtained from

$$h_{w2} = h_{w3} + N_2\, h_{wg3}$$

Calculated values are shown in figure 11 and $e_c$ values in figure 12.

Binary isobutane cycle

Another technology proposed to obtain electric power from geothermal fluid involves the use of a heat exchanger to transfer the energy to a working fluid such as isobutane, and this second fluid is used in the turbine. (see e.g., Cortez and others, 1973, Anderson, 1973, Mirk and

Wollenberg, 1974, Beaulaurier, 1974). The optimization of such a cycle involves the choice of many parameters such as the specific working fluid, the ratio of flow rate of working fluid to flow rate of primary-fluid, working pressure of secondary fluid, well pumping to keep primary fluid as a liquid versus flash eruption, and two-phase flow in the heat exchanger. The particular cycle chosen here involves pumped wells delivering liquid water to a heat exchanger, isobutane as the working fluid, equal flows of primary and secondary fluids, and work output optimized on working pressure of secondary fluid. A schematic diagram of the cycle is shown in figure 13 with numbers for one of the examples. Starting before the heat exchanger, compressed liquid isobutane is heated to superheated vapor at constant pressure, then passes to the turbine where it expands to produce 70% of the work of an isentropic process, passes to a heat exchanger where it is cooled to saturated liquid at 40°C, goes to a pump where the pressure is raised to the working pressure, and then starts the cycle again. An important part of analyzing binary cycles is what happens in the heat exchanger. The first problem is a trade-off between heat exchanger cost and temperature difference between the two fluids. I adopt the simplification that the isobutane is heated to within 11.1°C (20°F) of the hot-water source temperature and that the mass flows are equal. The second problem is that it is not always possible to satisfy this criterion because of the "pinch-point effect"; this can be understood by looking at the diagram on the bottom of figure 13 showing isobutane and water temperatures as a function of enthalpy change. The pinchpoint effect is caused by the enthalpy change needed for boiling the isobutane taking place at constant

isobutane temperature. This energy is supplied by transfer of heat from the water which then decreases in temperature. At the point where the isobutane is saturated liquid, the water temperature must be greater than the isobutane temperature. For lower temperature resources this criterion is critical, and I have assumed that the water is 2.8°C (5°F) above the isobutane temperature at the pinch-point. This assumption determines the isobutane temperature at the outlet of the heat exchanger rather than the earlier assumption for temperature difference.

Assuming a case where the pinch-point analysis is important, a source-water temperature and isobutane working pressure are chosen. The temperature of saturated isobutane $T_{fb}$ at that working pressure is obtained from the thermodynamic properties of isobutane (Canjar and others, 1963). The temperature of the water at point wa on the diagram in figure 13 is set at 2.8°C (5°F) above that. The enthalpy of isobutane at the outlet of the heat exchanger $h_{gc2}$ may be determined from an enthalpy balance written as

$$h_{gc2} = h_{fb} + (h_{wH1} - h_{wa}) \qquad (16)$$

where the enthalpies on the right hand side of equation (16) are known because the temperatures are known. The temperature $T_{gc2}$ is obtained by knowing the enthalpy calculated above and that the pressure is constant in the heat exchanger.

Whether the outlet isobutane temperature is determined by the above calculation or is simply set at 11.1°C (20°F) below the inlet water temperature, the following analysis applies. Starting before the pump, the isobutane is 40°C saturated liquid. The work done on the isobutane to take it from pressure $p_4$ to pressure $p_{fc}$ is approximately $V_{f4}(P_{fc1}$-

$P_4$), so the enthalpy at the inlet of the heat exchanger is

$$h_{fc1} = h_{f4} + V_{f4} (P_{fc1} - P_4). \quad (17)$$

The enthalpy of the water at the outlet is determined from an enthalpy balance on the heat exchanger, which may be written as

$$h_{wH2} = h_{wH1} - (h_{gc2} - h_{fc1}) \quad (18)$$

and the temperature may be then determined from the steam tables. The net work out of the turbine (removing the isobutane pump work) is

$$W_{act} = e_t [(h_{gc2} - h_{g3}) - V_{f4}(P_{fc1} - P_4)] \quad (19)$$

where $h_{g3}$ is found by assuming an isentropic expansion from gc2 to 5.3 bar (77 psia) and $e_t = 0.7$. The availability of the isobutane at state gc2 is

$$y = (h_{gc2} - T_o s_{gc2}) - (h_{f4} - T_o s_{f4}). \quad (20)$$

The whole procedure is then repeated for a different chosen working pressure until $W_{act}$ from equation (19) is maximized. Table 2 presents a summary of the cases which have been calculated. Values have also been plotted in figures 11 and 12. The last column presents values for the ratio $W_{act}/y$ as obtained from equations (19) and (20). Unlike the steam cycle where this ratio is fairly constant, the values for isobutane decrease with increasing temperatures. This reflects the fact that at higher temperatures the cycle involves an increasing degree of superheat which tends to decrease the fraction of Carnot efficiency that one is able to obtain. The net power continues to rise, but the cycle becomes poorer relative to a Carnot cycle. This naturally leads to conjectures that over certain temperature ranges other working fluids may be better suited than isobutane or that other more complicated cycles may be required than the one presented here (Chow and others, 1974)

Total flow

Another proposed new technology known as "Total Flow" is the expansion of steam-water mixtures through a nozzle to high velocities to drive an impulse turbine (Austin and others, 1973, Austin and Lundberg, 1974). The major point of this proposal is the use of the total flow of liquid and steam in the turbine. Various technical problems such as nozzle design, mineral deposition, etc. need to be resolved, but in principle it is possible to obtain quite high efficiencies. The following analysis is based on Austin and Lundberg (1974). Assuming an isentropic expansion in the well and nozzle, the mass fraction of steam at the entrance to the turbine may be written as:

$$N = (s_1 - s_{wo})/s_{wgo} \tag{21}$$

where $s_1$ is the entropy of the source fluid, $s_{wo}$ that of saturated liquid at the temperature $T_{wo} = 40°C$ and $s_{wgo}$ the entropy of phase change at $T_{wo}$. Defining a nozzle velocity coefficient $e_n$ as the fraction of theoretical velocity which a real nozzle attains, the kinetic energy at the turbine entrance is:

$$\frac{u^2}{2} = e_n^2 [h_1 - (h_{wo} + N h_{wgo})]. \tag{22}$$

Defining a wheel efficiency $e_w$ as the fraction of kinetic energy at the inlet which is obtained as useful work, the actual work is

$$W_{act} = e_w \frac{u^2}{2}$$

$$W_{act} = e_w e_n^2 [h_1 - (h_{wo} + N h_{wgo})]. \tag{23}$$

If the two coefficients are set equal to one, equation (23) yields numbers which are essentially the same as the availability calculation for hot water given above. Data for $e_w$ and $e_n$ are rather limited, but

Austin and Lundberg (1974) feel that a value of 0.9 should be obtainable for both parameters yielding a net reduction from the ideal of $(0.9)^3 = 0.73$. Values calculated on this basis are shown in figure 11. If these design variables can be met, the plot shows that the total flow method does offer significant gains in efficiency.

## PROCESS AND HOME HEATING

Where applicable, geothermal energy is especially attractive for supplying heat for industrial processes and for home heating. In these applications, the process dictates a desired temperature for the source of the heat and then some fraction of the heat above 15°C is used in the process (see Reistad, 1975 for a review of these considerations). For example, desired home temperatures are about 20°C. Water at 40°C could be used as the heat source and in theory give up all its energy above 20°C to the home. In practice, the economics of heat exchangers are such that 40°C water would probably yield only a few degrees of heat and would require new technology to do this economically. Under current technology, desired source temperatures are from 70 to 90°C with the water decreasing 10 to 20°C in temperature. For reference, short horizontal lines have been drawn on the energy axis of figure 11 and the efficiency axis of figure 12 for 150°C water giving up 10 to 20°C temperature drop. It is clear that even at this high temperature, the amount of usable energy which can be obtained from these conservative temperature drops is equal to or greater than that obtained as electrical power. At this high temperature, it still might make good sense to generate electrical power since it is so transportable whereas thermal energy is not very transportable. At temperatures on the order of 80 to 100°C, temperature

drops on the order of 10 to 20°C are still reasonable and the use of geothermal resources for their thermal energy becomes very attractive. In practice, transportation distances of 18 kilometers (Einarsson, 1973) and in theory to several tens of kilometers seem reasonable. A significant problem in home heating is the load factor. In Iceland, the climate is such that some heating is required year around so the yearly load factor is 57% (Einarsson, 1973). For application in the United States, load factors would be lower.

Other uses for process heat have been discussed by Reistad (1975) and current geothermal applications by Lindal (1973) and Einarsson (1970). The current range of applications are significantly below the potential described by Reistad. A review of current status and future prospects is being prepared by a subcommittee of The Committee on the Challanges of Modern Society and should better define the future directions of the non-electrical uses of geothermal resources.

## References Cited


Anderson, J. H., 1973, The vapor-turbine cycle for geothermal power generation: in Paul Kruger and Carel Otte [eds.]: Geothermal Energy: Resources, Production, Stimulation, Stanford Univ. Press, Stanford, California P. 163-175.

Austin, A. L., Higgins, G. H., and Howard, J. H., 1973, The total flow concept for recovery of energy from geothermal hot brine deposits: Lawrence Livermore Laboratory, UCRL-51366, 39 p.

Austin, A. L., and Lundberg, A. W., 1974, The total flow method for conversion of geothermal energy: Lawrence Livermore Laboratory, SDK 74-12, 28 p.

Axtmann, R. C., 1975, Environmental impact of a geothermal power plant: Science, v. 187, no. 4179, p. 795-802.

Banwell, C. J., 1963, Oxygen and hydrogen isotopes in New Zealand thermal areas: in Tongiorgi, E., Nuclear geology on geothermal areas, Pisa, Laboratorio di Geologia Nucleare, p. 95-138.

Beaulaurier, L. O., 1974, Binary thermodynamic power cycles applied to geothermal fluids: presented at the First Geothermal Implementation Conference, Committee on Challenges of Modern Society, Wairakei, New Zealand, 36 p.

Bodvarsson, G., 1969, On the temperature of water flowing through fractures: Jour. Geophys. Research, v. 74, no. 8, p. 1987-1992.

Bodvarsson, G., 1972, Thermal problems of siting of reinjection wells: Geothermics, v. 1, no. 2, p. 63-66.

Bodvarsson, G., 1974, Geothermal resource energetics: Geothermics, v. 3, no. 3, p. 83-92.

Boldizsar, T., 1963, Terrestrial heat flow in the natural steam field at Larderello: Geofisica Pura E Applicata - Milano, v, 56, p. 115-122.

Canjar, L. N., Nahmias, D., and Manning, F. S., 1963, Thermo properties of hydrocarbons - Part 7: Thermodynamic Properties of i-Butane: Hydrocarbon Process. Petrol. Refiner, v. 42, no. 8, p. 127.

Chou, J. C. S., Ahluwalia, R. K., and Woo, E. Y. K., 1974, Regenerative vapor cycle with isobutane as working fluid: Geothermics, v. 3, no. 3, p. 93-99.

Cortez, D. H., Holt, Ben, and Hutchinson, A. J. L., 1973, Advanced binary cycles for geothermal power generation: Energy Sources, v. 1, no. 1, p. 73-93.

Diment, W. H., Urban, T. C., Sass, J. H., Marshall, B. V., Munroe, R. J., and Lachenbruch, A. H., 1975, Temperature and heat contents based on conductive transport of heat: in White, D. E., and Williams, D. L., [eds.], Assessment of Geothermal Resources of the United States - 1975, U. S. Geol. Survey Circ. 726, p. 84-103.

Einarsson, S. S. 1970, Utilization of low enthalpy water (for space heating, industrial, agricultural and other uses): Geothermics, Special Issue 2, v. 1, p. 112-121.

_____, 1973, Geothermal district heating: in Armstead, H. C. H., [eds], Geothermal Energy: Review of Research and Development, Unesco, Paris, p. 123-134.

Finney, J. P., 1973, Design and operation of The Geysers Power Plant, in Kruger, Paul and Otte, Carel [eds.]: Geothermal Energy: Resources, Production, Stimulation, Stanford, Calif., Stanford Univ. Press, p. 145-161.

Fisher, R. G., 1964, Geothermal heat flow at Wairakei during 1958: New Zealand Jour. of Geology and Geophysics, v. 7, p. 172-184.

Gardner, G. H. F., Downie, J., and Kendall, H. A., 1962, Gravity segregation of miscible fluids in linear models: Soc. Petrol. Engineers Jour., p. 95-104.

Grindley, G. W., 1965, The geology, structure, and exploitation of the Wairakei geothermal field, Taupo, New Zealand: New Zealand Geological Survey Bulletin 75, 131 p.

Gringarten, A. C., Witherspoon, P. A., and Ohnishi, Yuzo, 1975, Theory of heat extraction from fractured hot dry rock: Jour. Geophys. Res., v. 80, no. 8, p. 1120-1124.

Haberman, B., 1960, The efficiency of miscible displacement as a function of mobility ratio: Petrol. Trans. AIME, v. 219, p. 264-272.

Harlow, F. H., and Pracht, W. E., 1972, A theoretical study of geothermal energy extraction: Jour. Geophys. Res., v. 77, no. 35, p. 7038-7048.

Hunt, T. M., 1970, Net mass loss from the Wairakei geothermal field, New Zealand: Geothermics, Special Issue 2, v. 2, pt. 1, p. 487-491.

James, R., 1967, Optimum wellhead pressure for geothermal power: New Zealand Engineering, 22, p. 221-228.

James, R., 1968, Pipeline transmission of steam-water mixtures for geothermal power: New Zealand Engineering, 23, p. 55-61.

Jones, G. B., and Hawkins, G. A., 1960, Engineering Thermodynamics, John Wiley, New York, 724 p.

Keenan, J. H., Keyes, F. G., Hill, P. G., and Moore, J. G., 1969, Steam tables. Thermodynamic properties of water including vapor, liquid, and solid phases: John Wiley, New York, 162 p.

Lindal, B., 1973, Industrial and other applications of geothermal energy, in Armstead, H. C. H., [ed.], Geothermal Energy: Review of Research and Development, Unesco, Paris, p. 135-148.

Mercer, J. W., Jr., Pinder, G. F., and Donaldson, I. G., 1975, A Galerkin-finite element analysis of the hydrothermal system at Wairakei, New Zealand: Jour. Geophys. Res., v. 80, no. 17, p. 2608-2621.

Mirk, K. F., and Wollenberg, H. A., 1974, The Lawrence Berkeley Laboratory geothermal program in northern Nevada: Lawrence Berkeley Laboratory 3224, 22 p.

Nathenson, Manuel, 1975, Some reservoir engineering calculations for the vapor-dominated systems at Larderello, Italy: U.S. Geol. Survey open-file rept., 75-142, 35 p.

Nathenson, Manuel and Muffler, L. J. P., 1975, Geothermal resources in hydrothermal convection systems and conduction-dominated areas: in White, D. E., and Williams, D. L., [eds.], Assessment of Geothermal Resources of the United States - 1975: U.S. Geol. Survey Circ., p. 104-121.

Raleigh, C. B., Witherspoon, P. A., Gringarten, A. C., and Ohnishi, Yuzo, 1974, Multiple hydraulic fracturing for the recovery of geothermal energy: [abs]: EOS, v. 55, no. 4, p. 426.

Ramey, H. J., Jr., 1970, A reservoir engineering study of The Geysers geothermal field: Evidence Reich and Reich, petitioners v. Commissioner of Internal Revenue, 1969, Tax Court of the United States, 52. T.C. No. 74, 1970.

Reistad, G. M., 1975, Analysis of potential nonelectrical applications of geothermal energy and their place in the national economy: Lawrence Livermore UCRL - 51747, 27 p.

Rosenhow, W. M. and Choi, H. Y., 1961, Heat, mass, and momentum transfer: New Jersey, Prentice-Hall, 537 p.

Truesdell, A. H., and White, D. E., 1973, Production of superheated steam from vapor-dominated reservoirs: Geothermics, v. 2, p. 145-164.

U.S. Bureau of Reclamation, 1974, Geothermal resource investigations - East Mesa Test Site - Status Rept., 64 p.

Urban, T. C., Jamieson, I. M., Diment, W. H., and Sass, J. H., 1975, Heat flow at The Geysers, California [abs.]: in Second United Nations Symposium on the Development and Use of Geothermal Resources.

White, D. E., Muffler, L. J. P., and Truesdell, A. H., 1971, Vapor-dominated hydrothermal systems compared with hot-water systems: Econ. Geology, v. 66, p. 75-97.

Table 1.--Conduction length as a function of time for a thermal diffusivity of 23.2 $m^2/yr$.

| Time (years) | 1 | 5 | 10 | 15 | 20 | 25 | 30 |
|---|---|---|---|---|---|---|---|
| Conductive length (metres) | 19 | 43 | 61 | 75 | 86 | 96 | 106 |

Table 2.--Summary of calculations for the isobutane cycle

| Water inlet temperature in °C | Water outflow temperature in °C | Isobutane inlet temperature in °C | Isobutane outlet temperature in °C | Isobutane pressure at turbine inlet, bars | Net Work $\frac{\text{k.w.s.}}{\text{kg}}$ | $\frac{w_{act}}{y}$ |
|---|---|---|---|---|---|---|
| 150 | 61.7 | 41 | 102 | 20.7 | 33 | 0.67 |
| 176.7 | 61.7 | 42 | 160 | 34.5 | 58 | 0.61 |
| 204.4 | 76.7 | 43 | 193.3 | 48.3 | 70 | 0.55 |
| 250 | 102.5 | 44 | 239 | 69.0 | 87 | 0.50 |
| 300 | 145 | 47 | 289 | 137.9 | 110 | 0.47 |

Mass flows of isobutane and water assumed equal. Isobutane assumed to expand isentropically through turbine to 5.3 bar pressure and to be cooled isobarically to 40°C before going through a pump. Isobutane leaves heat exchanger at 11.1°C below water inflow temperature except where pinch point analysis assumption of 2.8°C minimum temperature difference in heat exchanger dictates different condition.

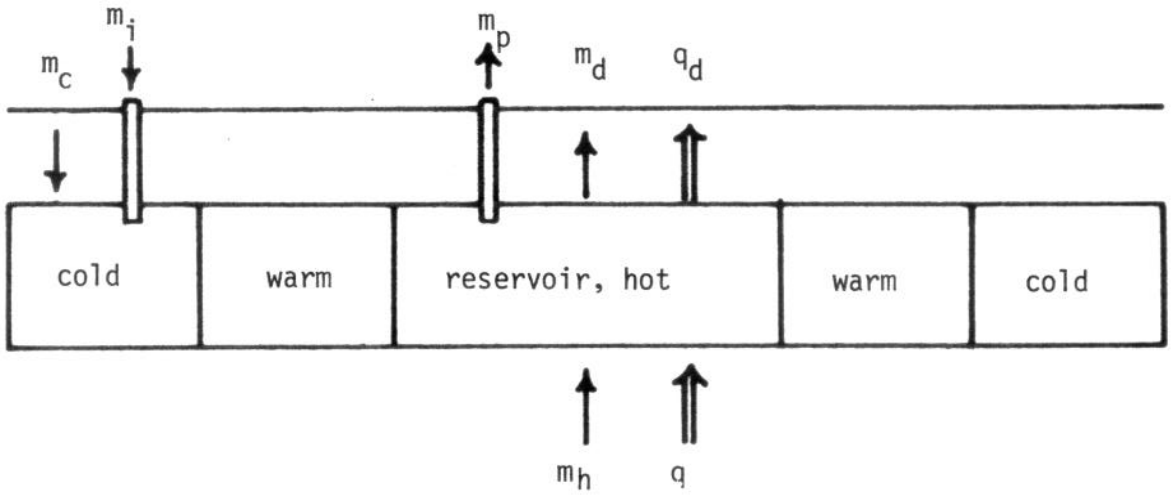


Figure 1.--Schematic of a geothermal reservoir showing heat recharge by conduction q and the flow of hot-water $m_h$. Fluids are produced at the rate $m_p$ and injected at rate $m_i$. A natural flow of cold recharge $m_c$ is also shown. The flows $m_c$, $m_h$ and $q$ may be affected by production to an unknown extent.

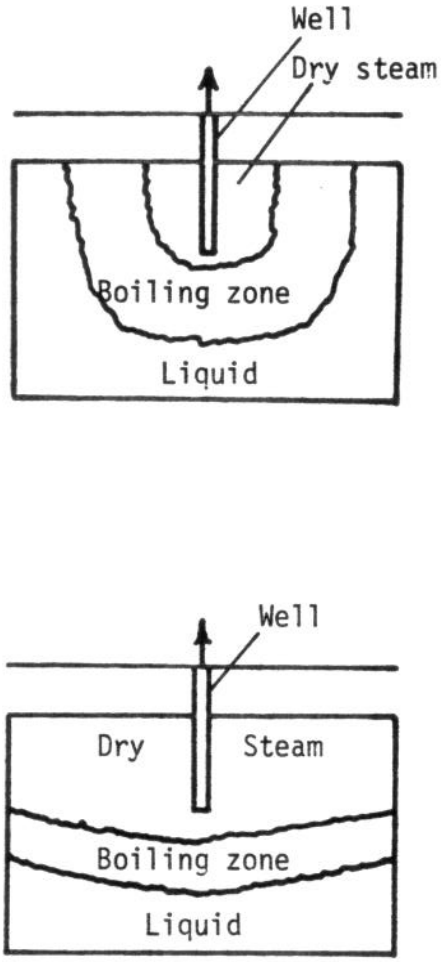


Figure 2.--Conceptual models of boiling fronts in ideal closed-volume hot-water reservoirs. Top is early time situation as front propagates from well. Bottom figure shows situation at a later time when gravity segregation has caused boiling front to become approximately horizontal.

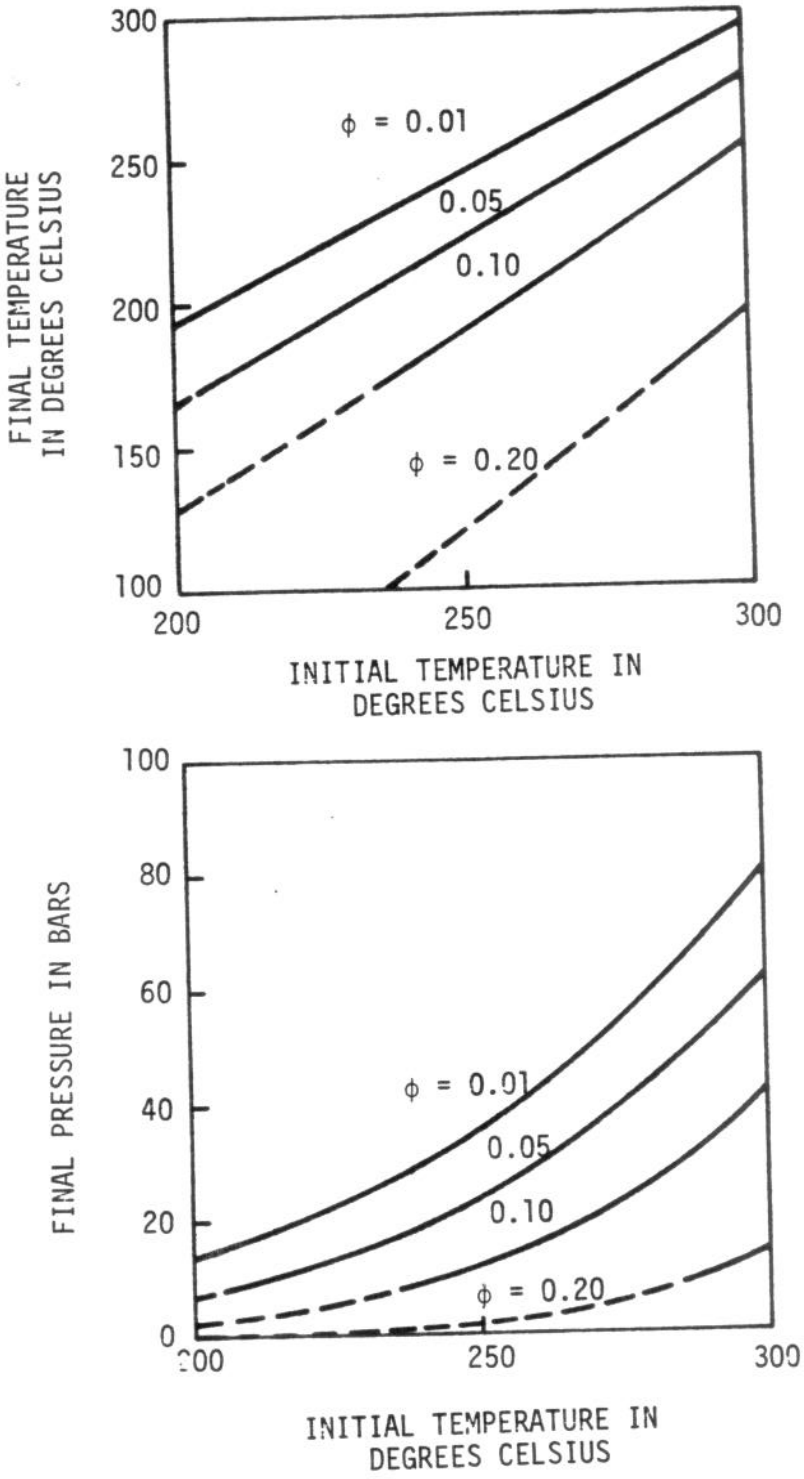


Figure 3.--Relations between initial and final states across a boiling zone, proceeding from saturated liquid to saturated vapor with porosity $\phi$ as a parameter. Dotted parts of curves show where final pressure is less than 8 bars absolute.

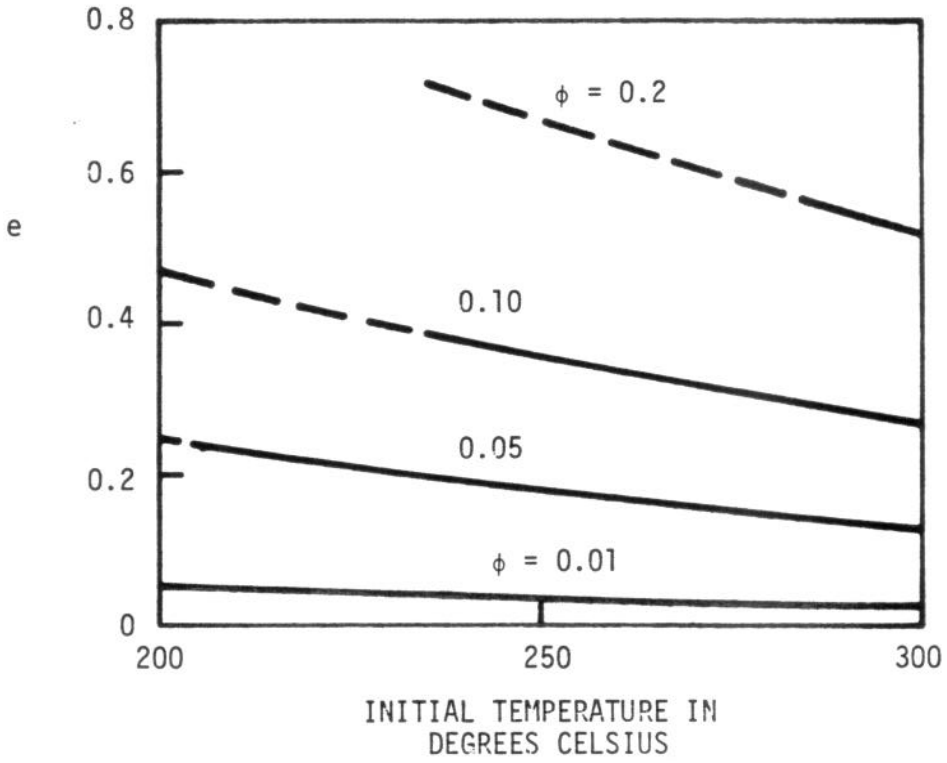


Figure 4.--Fraction e of stored thermal energy above 15°C obtained at the surface in a system exploited by boiling to steam. Curves broken where steam pressure is less than 8 bars absolute.

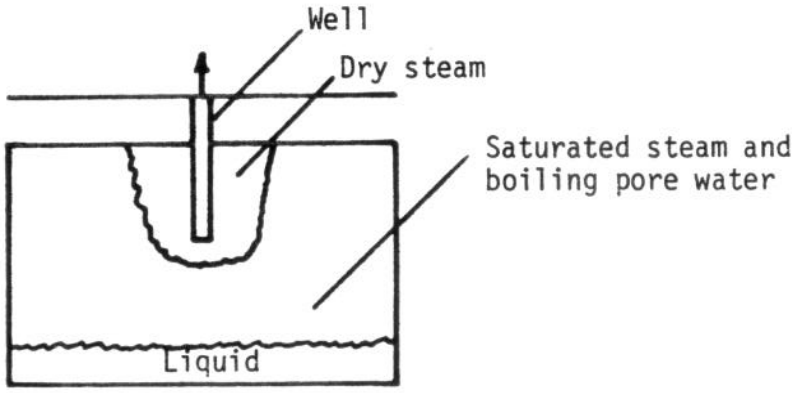


Figure 5.--Conceptual model of vapor-dominated reservoir showing dried zone around well, boiling of immobilized pore water, and inferred boiling deep water-table.

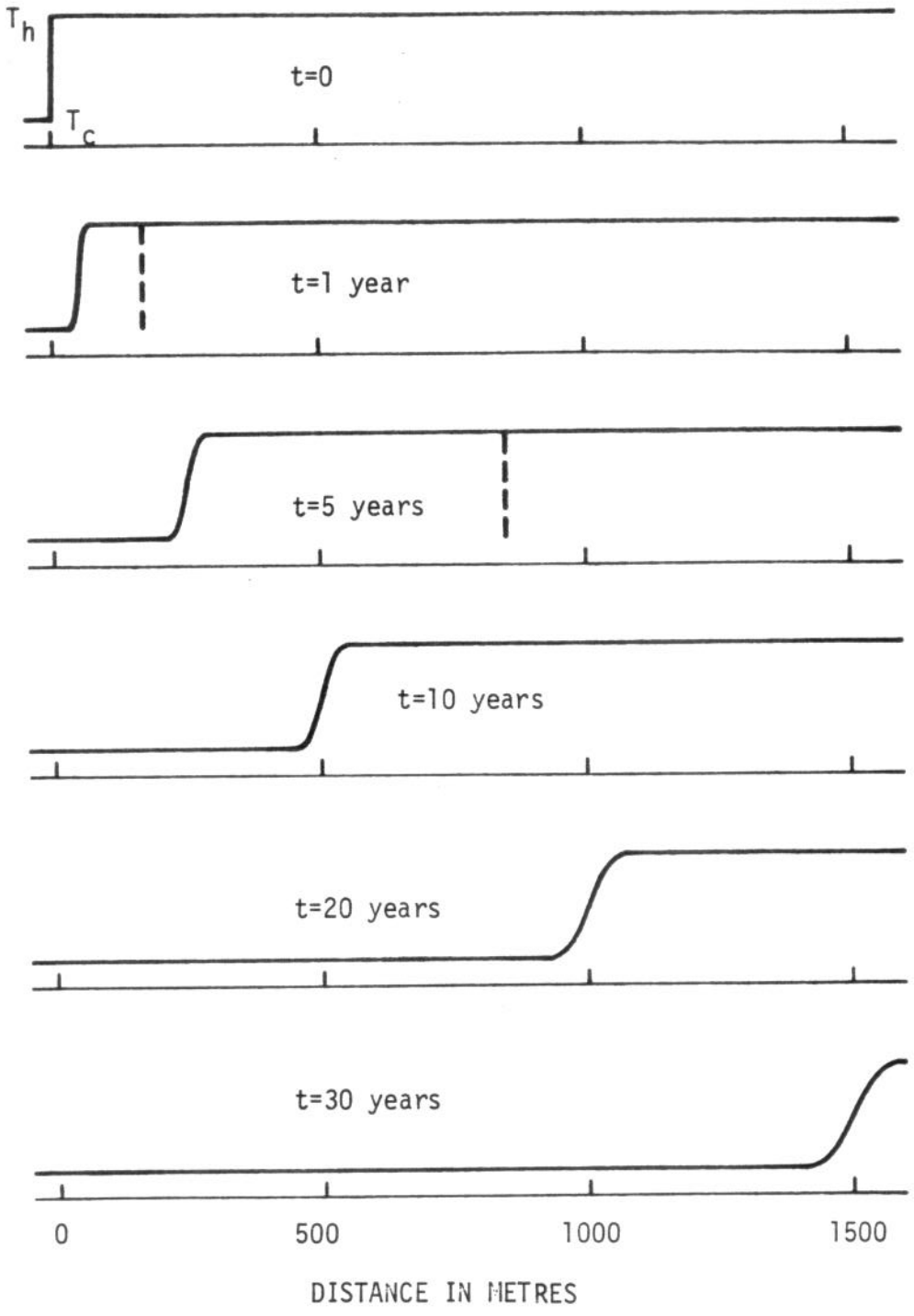


Figure 6.--Temperature as a function of distance at various times for cold water being injected into a hot porous medium (porosity = 0.2). Vertical dashed lines show location of chemically tagged water which started at x=0 at t=0.

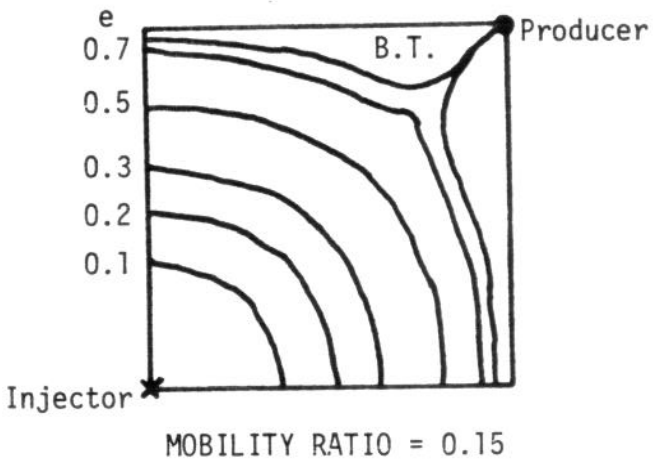


MOBILITY RATIO = 0.15

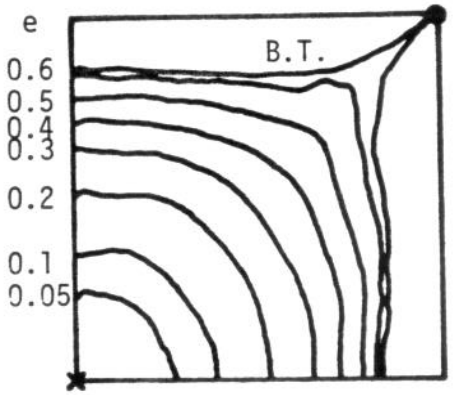


MOBILITY RATIO = 1.0

Figure 7.--One fourth of a five spot cold water drive based on miscible displacement data of Haberman (1960). Numbers are fraction of stored energy recovered when cold water front is at location shown neglecting conduction. B.T. denotes position of front at breakthrough. (Figures courtesy of Society of Petroleum Engineers of AIME).

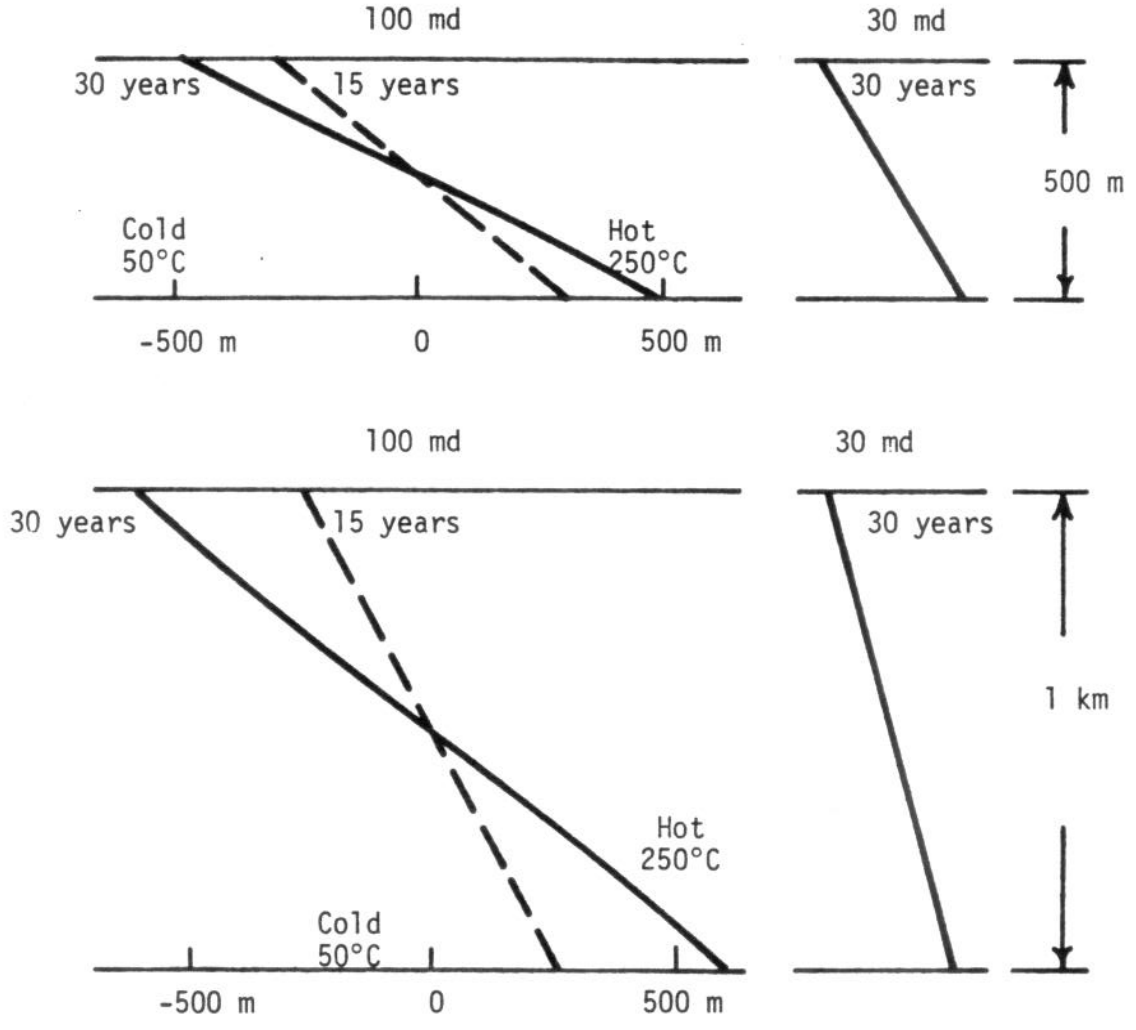


Figure 8.--Gravity segregation in miscible displacement due to density difference between cold and hot water for an initially vertical front with no net through flow. Vertical and horizontal are same scale.

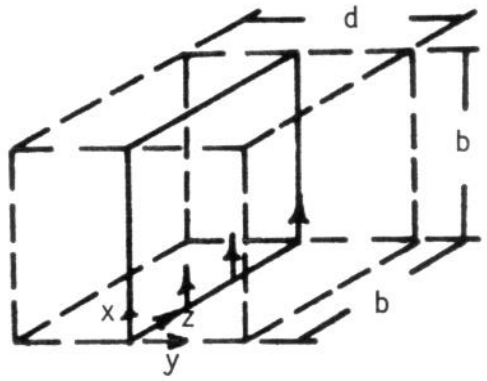


Figure 9.--Schematic for solution of conduction problem of a planar crack with water flowing uniformly upward. Average spacing between cracks is d.

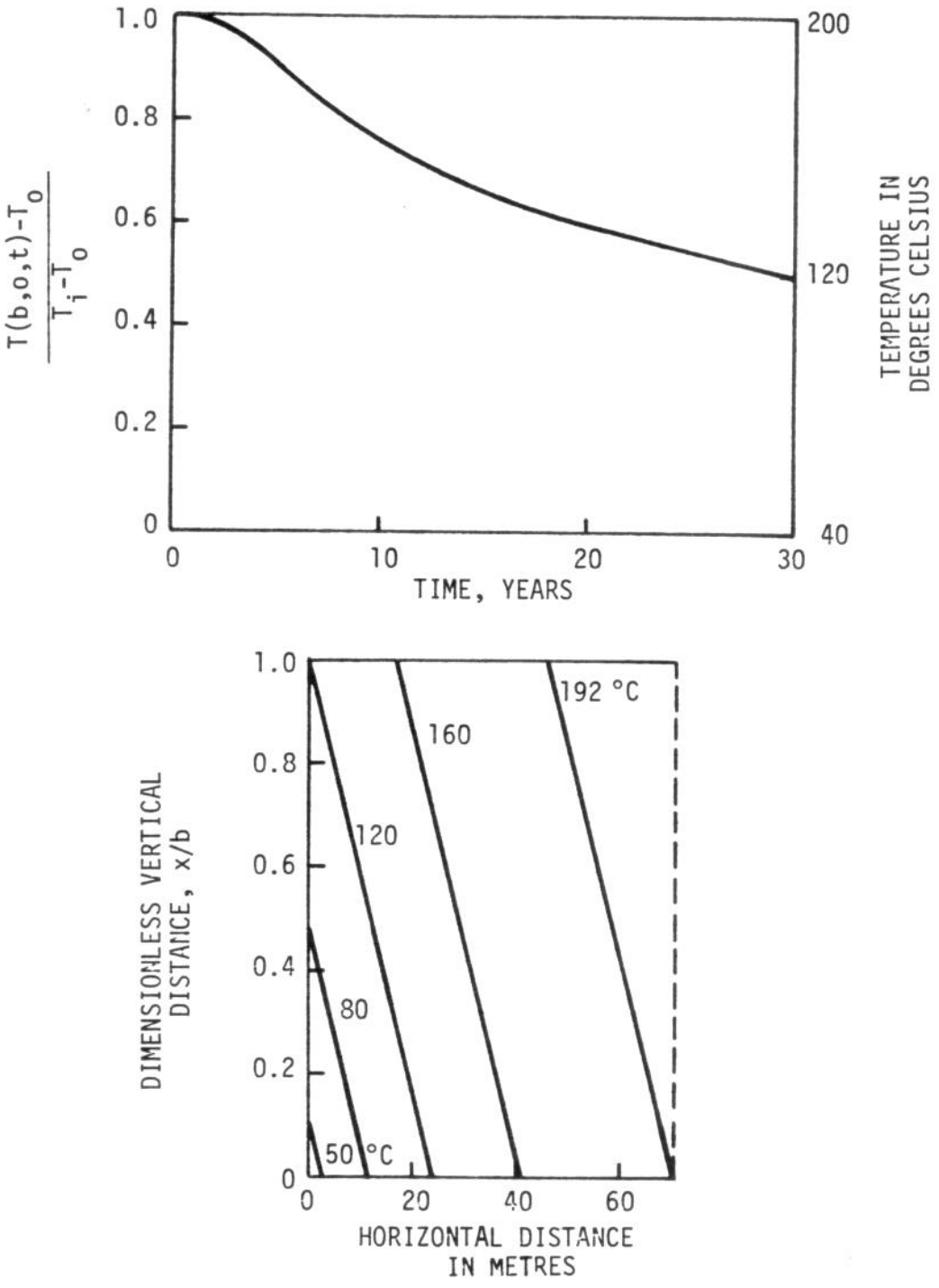


Figure 10.--Temperatures in the crack as a function of time (top) and in the rock to the right of the crack at the end of 30 years (bottom). Vertical dimension in bottom figure is dimensionless height and horizontal dimension is actual distance. Actual geometry is thin and high compared to drawing.

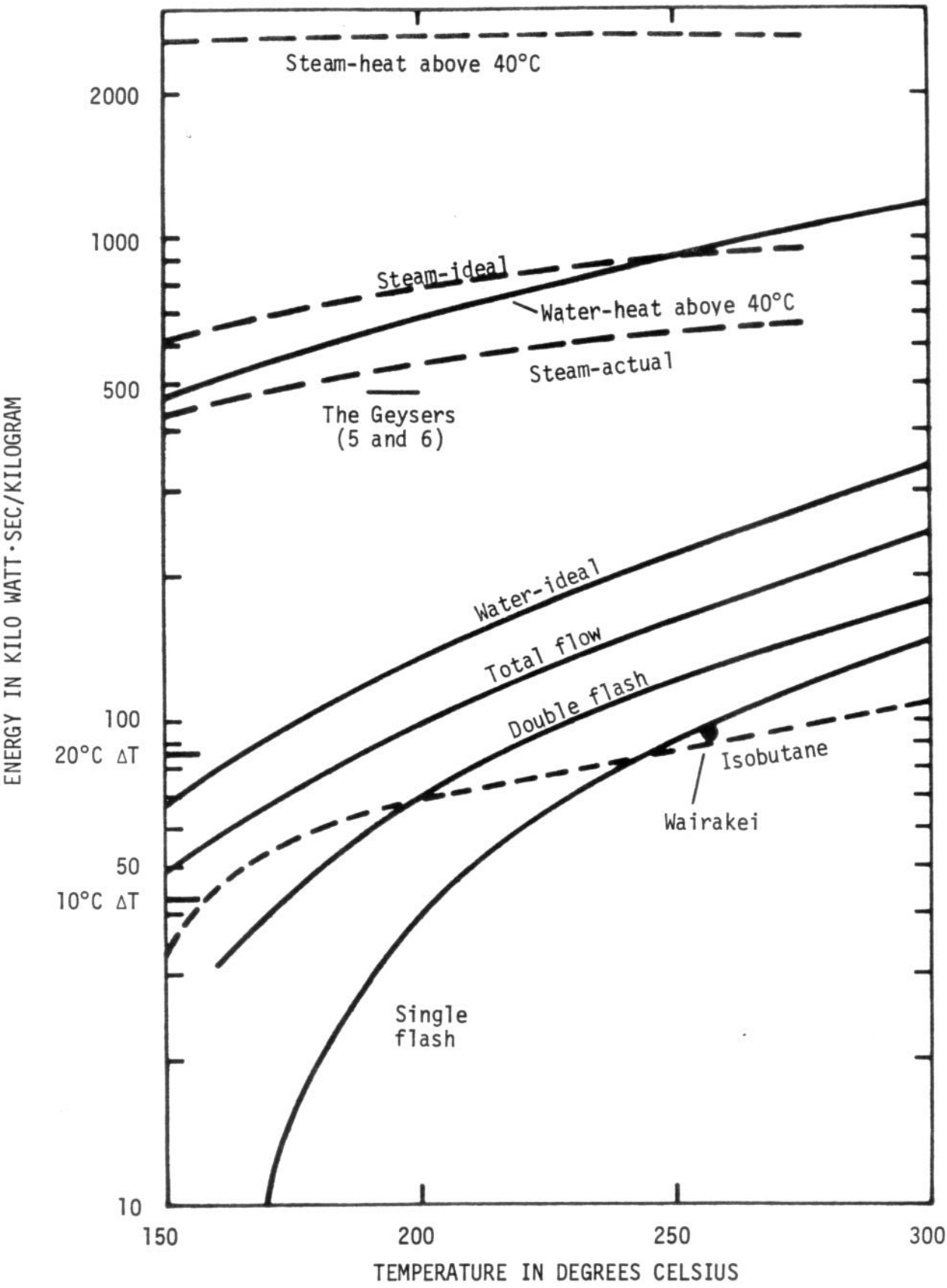


Figure 11.--Heat above 40°C, ideal work, and actual work as a function of source temperature. Energy obtained from 10 and 20°C temperature drop in process-heat application shown on energy axis.

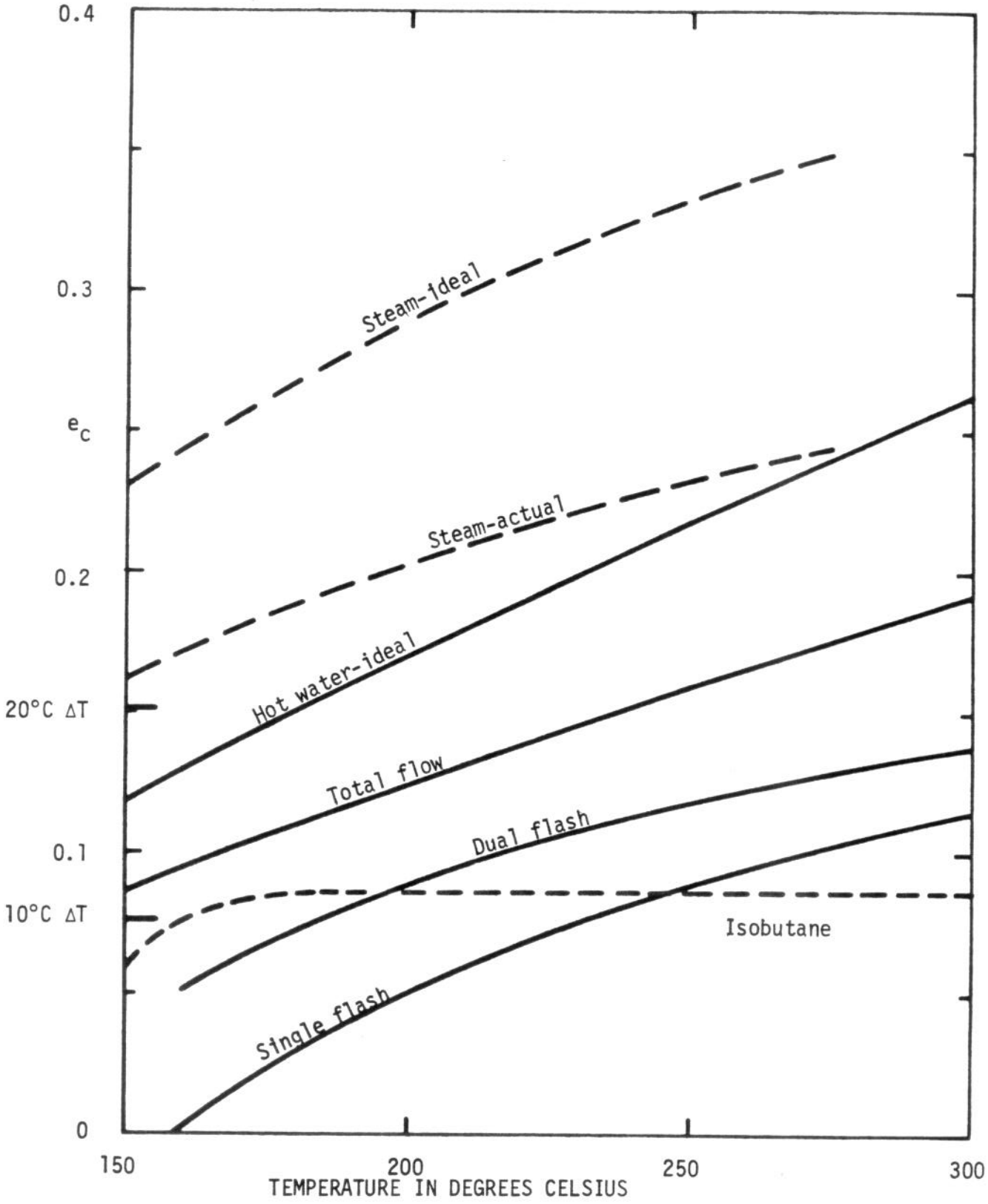


Figure 12.--Quantity $e_c$ defined as work or availability divided by enthalpy of source fluid above 15°C reference enthalpy as a function of source temperature. Conversion efficiency for 10 and 20°C temperature drop in process-heat application shown on $e_c$ axis.

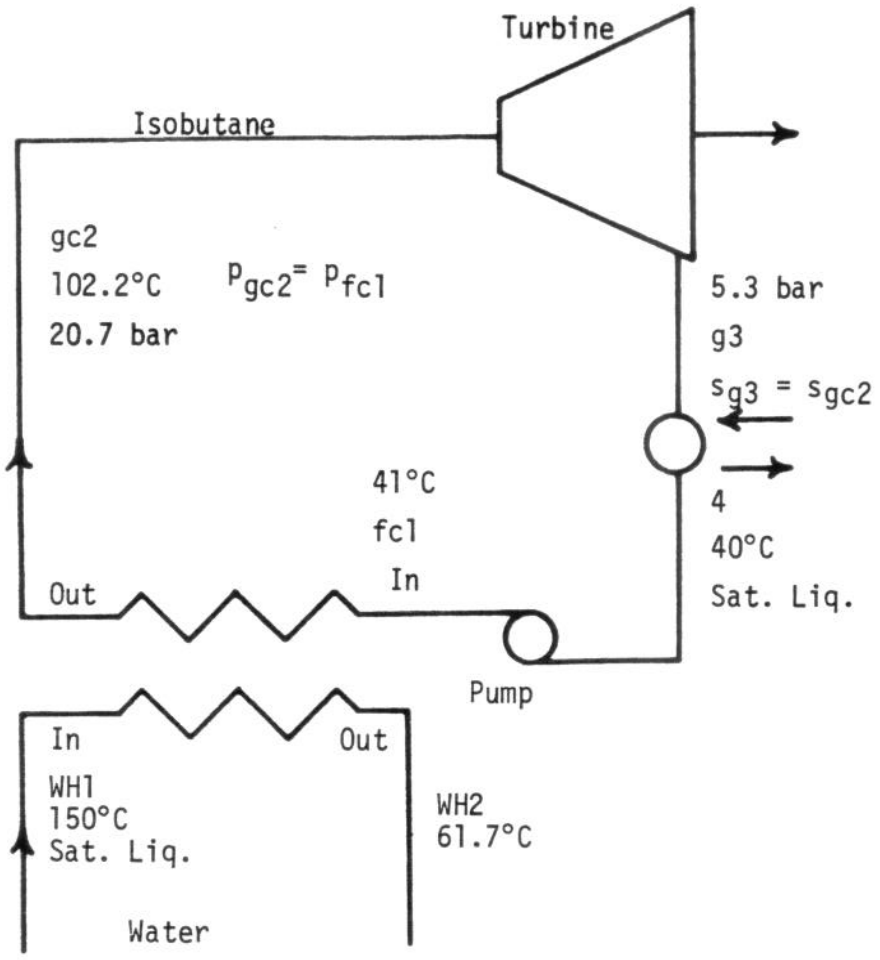


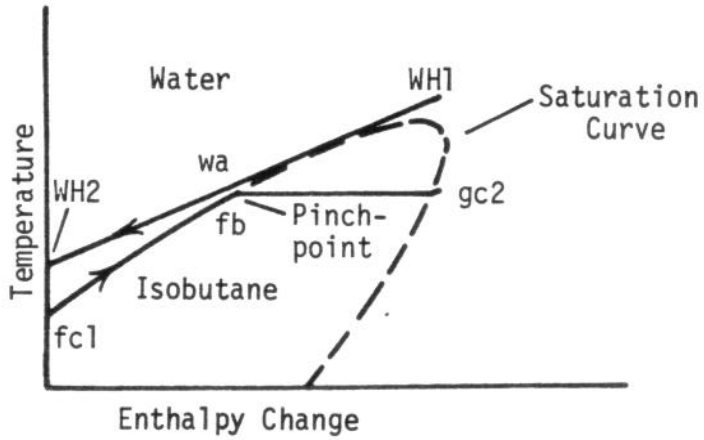


Figure 13.--Cycle diagram for binary isobutane system (top) and temperature-enthalpy diagram for heat exchanger (bottom).